




Modeling the influence of COVID-19 protective measures on the mechanics of phonation^{a)}

Jonathan J. Deng,¹ Mohamed A. Serry,¹ Matías Zañartu,²  Byron D. Erath,³  and Sean D. Peterson^{1,b)} 

¹Mechanical and Mechatronics Engineering, University of Waterloo, Waterloo, Ontario N2L 3G1, Canada

²Department of Electronic Engineering, Universidad Técnica Federico Santa María, Valparaíso, Chile

³Mechanical and Aerospace Engineering, Clarkson University, Potsdam, New York 13699, USA

ABSTRACT:

In an effort to mitigate the 2019 novel coronavirus disease pandemic, mask wearing and social distancing have become standard practices. While effective in fighting the spread of the virus, these protective measures have been shown to deteriorate speech perception and sound intensity, which necessitates speaking louder to compensate. The goal of this paper is to investigate via numerical simulations how compensating for mask wearing and social distancing affects measures associated with vocal health. A three-mass body-cover model of the vocal folds (VFs) coupled with the sub- and supraglottal acoustic tracts is modified to incorporate mask and distance dependent acoustic pressure models. The results indicate that sustaining target levels of intelligibility and/or sound intensity while using these protective measures may necessitate increased subglottal pressure, leading to higher VF collision and, thus, potentially inducing a state of vocal hyperfunction, a progenitor to voice pathologies.

© 2022 Acoustical Society of America. <https://doi.org/10.1121/10.0009822>

(Received 16 December 2021; revised 24 February 2022; accepted 27 February 2022; published online 3 May 2022)

[Editor: James F. Lynch]

Pages: 2987–2998

I. INTRODUCTION

Prophylactic measures imposed to mitigate the spread of severe acute respiratory syndrome coronavirus 2 (SARS-CoV-2), the virus responsible for the coronavirus disease (COVID-19), have significantly changed the lifestyle of the world's population. Two primary protective measures have been prescribed to the public to minimize the transmission of SARS-CoV-2, namely, wearing a face mask and social distancing. Wearing a mask aims to suppress the spread of droplets and aerosols generated during sneezing, coughing, and breathing, which transport virions (Agrawal and Bhardwaj, 2020; Khosronejad *et al.*, 2020; Mittal *et al.*, 2020; Shah *et al.*, 2021), while social distancing aims to maintain interindividual spacing beyond the distance that contaminated droplets and aerosols are thought to travel during common expiratory events (Xie *et al.*, 2007). These protective measures have proven effective in lowering the transmission rate of SARS-CoV-2 (Eikenberry *et al.*, 2020; Qian and Jiang, 2022). It should be noted that despite the quick development and availability of COVID-19 vaccines (Ndwandwe and Wiysonge, 2021), protective measures are likely to remain in place for a long period of time to mitigate the spread of the virus and its rapidly emerging variants (Koyama *et al.*, 2020).

Although effective in mitigating the spread of SARS-CoV-2, both social distancing and masks negatively impact

verbal communication, generally necessitating individuals to speak louder to compensate for the undesired effects of these protective measures. Masks have been characterized as low-pass filters (Corey *et al.*, 2020) that attenuate the high frequency content of speech signals, leading to reduced speech perception and intelligibility (Saunders *et al.*, 2021). Further contributing to the deterioration of intelligibility when wearing opaque masks is the loss of information embedded in lip movement cues that contribute to the audiovisual integration of speech intelligibility and nonverbal communication (Carbon, 2020; Mheidly *et al.*, 2020).

Because there is negligible atmospheric absorption between typical speaker/listener pairs (Attenborough, 2014; Evans *et al.*, 1972; ISO, 1993), social distancing more uniformly attenuates all frequencies of the speech signal with the amplitudes of all frequencies being inversely proportional to the distance between the speaker and receiver (Kinsler *et al.*, 1999); thus, the speaker must speak louder to produce the same sound pressure level (SPL) at the extended distance. Compensating for these effects may result in an increased vocal effort to sustain effective communication, such as that reported by healthcare workers during the pandemic (McKenna *et al.*, 2021). In the long run, increased vocal effort is a factor leading to hyperfunctional voice disorders (Hillman *et al.*, 2020). Similarly, the additional effort to “project your voice” in performers and teachers in comparison with the general population is believed to be the primary factor driving the larger prevalence of voice disorders in these populations (Guss *et al.*, 2014; Roy *et al.*, 2004).

^{a)}This paper is part of a special issue on COVID-19 Pandemic Acoustic Effects.

^{b)}Electronic mail: peterston@uwaterloo.ca

The underlying biomechanics of normal and pathological human phonation are often studied using numerical models (Galindo *et al.*, 2017; Ishizaka and Flanagan, 1972; Jiang *et al.*, 1998; Steinecke and Herzel, 1995; Story and Titze, 1995; Zañartu *et al.*, 2014). Such analyses can provide useful insight into the underlying mechanisms of vocal disorders. For example, Sommer *et al.* (2012, 2013) and Steinecke and Herzel (1995) investigated vocal fold (VF) oscillations using asymmetric two-mass models and found that imbalances between the right and left VFs can lead to chaotic VF oscillations; similar chaotic patterns were found when modeling unilateral polyps (Zhang and Jiang, 2004). Galindo *et al.* (2017) investigated the influence of a posterior glottal opening on the quality of voice using a triangular body-cover model (BCM) and found that compensating for deterioration in some voice measures associated with a posterior glottal opening leads to an increase in the VF collision pressure, which can lead to phonotrauma. Dejonckere and Kob (2009), using a three-dimensional multi-mass VF model, deduced that curved VFs and incomplete glottal closure, which are relatively more common in female speakers, necessitate increased subglottal pressure to compensate, leading to higher localized mechanical stress during phonation. Clinically, these results are correlated with an increased prevalence of nodules in female speakers.

As the use of protective face masks and social distancing have become common as a result of COVID-19, the long term consequences of these protective measures on the vocal health of individuals are presently out of the reach of clinical and experimental investigations due to the lack of long term data. However, enlisting a combination of numerical simulations and knowledge gleaned from functionally similar clinical

investigations may offer insights into the long term effects of COVID-19 protective measures on vocal health.

The goal of this paper is to explore, by means of numerical phonation simulations, the relative and combined impacts of wearing masks¹ and social distancing on vocal effort and VF collision forces. In particular, the focus of this study is to elucidate how the reduction in speech perception associated with these measures can potentially lead to vocal hyperfunction through compensatory mechanisms (Hillman *et al.*, 1989, 2020). The organization of this paper is as follows: Section II introduces the phonation and acoustic models; Sec. III elaborates on the study design; the acoustic effects of wearing masks and social distancing on several voice measures are investigated in Secs. IV and V, respectively; compensatory measures and the resulting implications for VF collision forces are investigated in Sec. VI; practical suggestions for maintaining vocal health while wearing a mask and engaging in social distancing are given in Sec. VII; Sec. VIII describes the limitations of the study; and Sec. IX concludes the work.

II. NUMERICAL PHONATION MODEL

A. Body-cover VF model

This study employs the BCM of the VFs (Story and Titze, 1995; Titze and Story, 2002), shown in the center of the top schematic in Fig. 1. This model, which embeds the essential physiological components of the VFs used in modal voice, consists of two cover masses and a body mass, denoted by m_l , m_u , and m_b , respectively. For the remainder of the manuscript, the subscripts “l,” “u,” and “b” will denote “lower” (inferior), “upper” (superior), and “body,” respectively. The

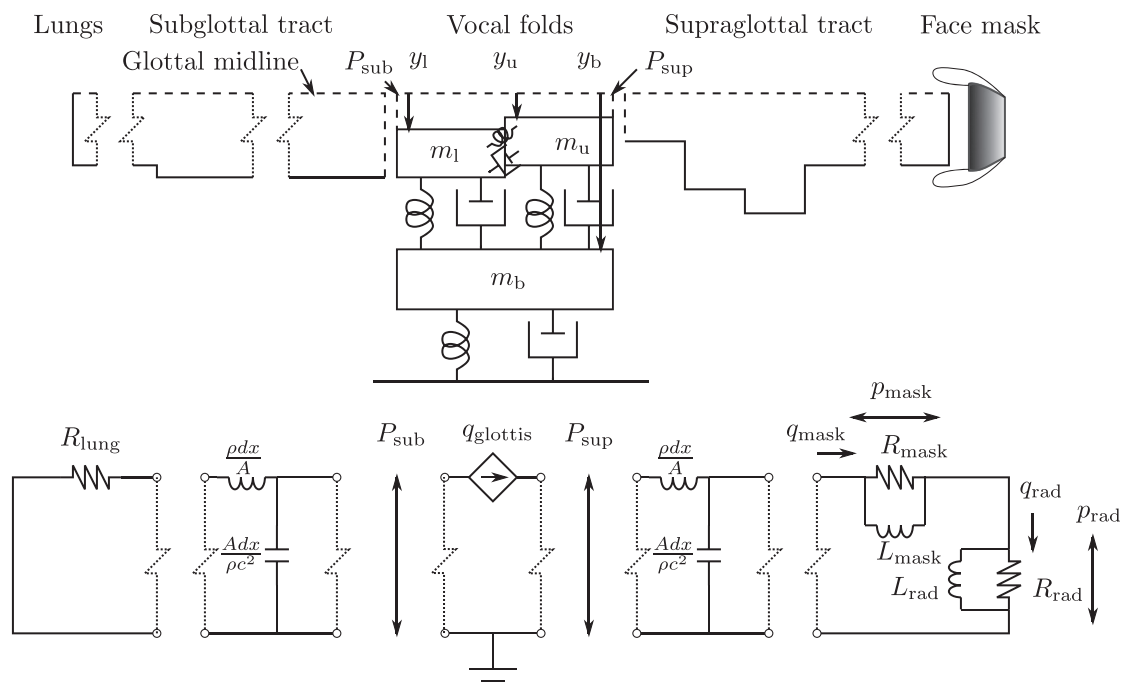


FIG. 1. A schematic diagram of the phonation model consisting of the BCM coupled with subglottal and supraglottal tracts (top) and a simplified circuit analogy representation of the model (bottom).

body and cover masses are interconnected and the body layer is connected to the fixed rigid larynx via springs and dampers to model the tissue viscoelasticity. Displacements of the masses from the medial plane are given by y_l , y_u , and y_b . It is assumed that both of the VFs have identical properties and their motions are symmetric about the medial plane. A collision of the opposing fold is modeled by applying additional nonlinear spring forces to the cover masses, which are proportional to the degree of overlap as the VFs cross the medial (collision) plane. Muscle activation rules are incorporated to control the primitive model variables (Titze and Story, 2002), wherein the muscle activation parameters a_{CT} , a_{TA} , and a_{LCA} , account for the activation of the cricothyroid (CT), thyroarytenoid (TA), and lateral cricoarytenoid/posterior cricoarytenoid (LCA/PCA) muscles, respectively.

B. Glottal flow and acoustics

The glottal flow and pressure forces on the VFs are computed according to a Bernoulli-based flow model, where flow separation is located at the junction between the lower and upper cover masses when the VF configuration is convergent and at the inlet of the glottis when the configuration is divergent (Story and Titze, 1995). The glottal flow is driven by the subglottal and supraglottal pressures that consist of static P and acoustic p components, such that the subglottal pressure is given by $P_{sub} + p_{sub}$ and the supraglottal pressure is given by $P_{sup} + p_{sup}$. The static components correspond to the equilibrium pressure conditions in the subglottal and supraglottal tracts when the VFs are at rest and fully adducted (i.e., P_{sub} and P_{sup} correspond to the lung and atmospheric pressures, respectively, in the case of equilibrium), whereas the acoustic components correspond to the perturbations in the pressure field due to travelling pressure waves. The coupling between the acoustic subglottal and supraglottal pressures and the glottal flow is performed using a modified (and sign corrected) version of the flow rate relation introduced by Titze (1984) (see Lucero and Schoentgen, 2015). The BCM equations are discretized in time using the Taylor series method (Galindo et al., 2014), which has been employed in several previous BCM studies (Galindo et al., 2017; Galindo et al., 2014; Hadwin et al., 2016; Serry et al., 2021).

The subglottal and supraglottal acoustic tracts are coupled with the BCM, and the acoustic wave propagation is modeled using the wave reflection analog (WRA) method (Kelly and Lochbaum, 1962; Liljencrants, 1985; Story, 1995, 2005). The losses are modeled using attenuation factors (Titze and Alipour, 2006; Zañartu, 2006) of the form $\alpha = 3.8 \times 10^{-3}l/\sqrt{A}$ for the supraglottal tract and $\alpha = 11.2 \times 10^{-3}l/\sqrt{A}$ for the subglottal tract, where A and l are the cross-sectional area and length of a given WRA tube section, respectively. The simulation time step is governed by the lengths of the WRA tube sections used in the tracts. Here, the supraglottal area functions corresponding to vowels /a/, /e/, /i/, /o/, and /u/ with section lengths of 0.25 cm are adopted from Takemoto et al. (2006) with a corresponding time step of 7.14×10^{-6} s, and

the vowel /æ/ with a section length of 0.396825 cm is adopted from Story et al. (1998) with a resulting simulation time step of 1.13×10^{-5} s. Similar to Galindo et al. (2014) and Zañartu et al. (2014), the subglottal tract area function is adapted from the respiratory system measurements of human cadavers (Weibel, 1963), covering only the trachea and bronchi. This tract consists of two tubes, where the lung side tube is nominally 4 cm long with a cross-sectional area of 2.33 cm^2 , and the glottis side tube is nominally 11 cm long with a cross-sectional area of 2.54 cm^2 . For a section length of 0.25 cm, this results in a total subglottal tract length of 15.75 cm, whereas for a section length of 0.396825 cm, this results in a total length of 15.873 cm. At the lung and mouth ends of the subglottal and supraglottal tracts, respectively, the continuities of the pressure and flow with an acoustic circuit model are enforced as boundary conditions. The lung termination circuit is modeled by a single resistor to ensure a reflection coefficient of -0.8 based on the boundary condition used by Zañartu et al. (2007) and shown schematically in Fig. 1.

In the absence of a mask, radiation from the mouth is modeled using the well-known approximation of a cylinder in an infinite baffle, which results in a parallel resistor-inductor (R-L) circuit (Flanagan et al., 1975; Story, 1995).

The acoustic effects of the mask are modeled as a parallel R-L acoustic circuit. The adopted mask model is based on the models for textile materials, where the effects of the flow through the fabric and movement of the fabric due to the acoustic pressures are considered (Moholkar and Warmoeskerken, 2003; Pieren, 2012). The total flow rate and pressure across the mask are given by

$$q_{\text{mask}} = q_{\text{mask},1} + q_{\text{mask},2},$$

$$p_{\text{mask}} = R_{\text{mask}}q_{\text{mask},1} = L_{\text{mask}}\frac{dq_{\text{mask},2}}{dt}, \tag{1}$$

where p_{mask} is the pressure drop across the mask, q_{mask} is the total flow rate across the mask, $q_{\text{mask},1}$ is the flow rate through the mask when the mask mass is infinite (or the mask mass is at rest), $q_{\text{mask},2}$ is the flow rate due to the mask movement, R_{mask} is the mask resistance, and L_{mask} is the mask inductance. In addition, to specify the intrinsic properties of the mask fabric, we define the scaled mask resistance and inductance (area density) as $r_{\text{mask}} = R_{\text{mask}}/A_t$ and $\rho_{\text{mask}} = L_{\text{mask}}/A_t$, respectively, where A_t is the terminal area at the mouth. These properties are independent of the size of the mask because they relate the pressure drop across the mask to the acoustic velocity through the mask rather than the flow rate.

The mask parameters R_{mask} and L_{mask} represent the resistance to the flow through the mask and inertia of the mask, respectively. Increasing the mask flow resistance would require increasing the pressure at the lungs to drive the same amount of air through and would, thus, be perceived as less breathable. Increasing the mask inertia would be felt as a heavier mask.

The mask circuit is connected in series with the mouth radiation circuit as the total flow rate through the mask is

also the radiated flow rate. The acoustic termination conditions are implemented numerically following the approach of Story (1995, Chap. 2). Specifically, the termination circuit is discretized in time with the bilinear transform, and the continuity of the pressure and flow between the termination circuit and the tract are applied to solve for the reflected pressures.

C. Far-field distance dependent pressure

The influence of social distancing on acoustic signals is considered by adopting the far-field wave approximation for the piston-in-baffle source (Kinsler *et al.*, 1999, Sec. 7.4).

Let q_{rad} be a T periodic signal, and let $\{q_{\text{rad},m}\}_{m=0}^{N-1} = \{q_{\text{rad}}(t_m)\}_{m=0}^{N-1}$ be the flow rate signals sampled with N points such that $N/f_s = T$ and f_s is the sampling frequency (N is even). The sampled flow rate can then be represented by one-sided discrete Fourier transform coefficients as

$$q_{\text{rad},m} = \sum_{n=0}^{N/2} \text{Re}\{\mathbf{q}_{\text{rad},n} e^{j\omega_n t_m}\}, \quad (2)$$

where $\mathbf{j} = \sqrt{-1}$, and $\omega_n = 2\pi f_s n/N$ and $\mathbf{q}_{\text{rad},n}$ are the associated modal frequencies and Fourier series coefficients, respectively. The bold font denotes a complex quantity. Then, the far-field acoustic pressure, p_f , in the frequency and time domains is given by

$$\mathbf{p}_{f,n}(d) = \frac{\mathbf{j}}{2} \rho c \frac{\mathbf{q}_{\text{rad},n}}{\pi d} k_n e^{-jk_n d}, \quad (3)$$

$$p_{f,m}(d) = p_f(d, t_m) = \sum_{n=0}^{N/2} \text{Re}\{\mathbf{p}_{f,n}(d) e^{j\omega_n t_m}\}, \quad (4)$$

where d is the distance from the mouth, t is the time, ρ is the air density, c is the speed of sound, and $k_n = \omega_n/c$ is the angular wave number. Lastly, for the numerical computation of the Fourier coefficients, we apply a Tukey window to q_{rad} with a tapered region fraction of 0.2 to avoid spectral leakage, which causes spurious high frequency content.

We note that Eq. (3) is limited because the frequency dependent energy-dissipative effects are present for sound propagation over long distances (Evans *et al.*, 1972; ISO, 1993). For the small distances in social distancing observed here, however, these effects will be negligible. For example, at a mid-band frequency of 10 kHz, 20° C, relative humidity of 15%, and ambient pressure of 1 atm, the sound attenuation due to the atmospheric absorption at a distance of 1 m is approximately 0.267 dB (ISO, 1993, Table 1) and even less at lower frequencies.

III. STUDY DESIGN

Simulations are performed for vowel phonemes /a/, /i/, /e/, /o/, /u/, and /æ/. Each simulation spans 1 s of phonation with the last 0.5 s considered in the analysis so as to eliminate the transient effects. An “average vowel” is computed by performing a weighted average of the individual vowels

according to the vowel frequency data reported by Hayden (1950) to roughly approximate running speech. Specifically, the average vowel comprises 15.7% /a/, 16.9% /e/, 14.5% /i/, 13.0% /o/, 13.2% /u/, and 26.9% /æ/. In all of the simulations, the laryngeal muscle activation parameters are set to $a_{\text{CT}} = a_{\text{TA}} = 0.2$ and $a_{\text{LCA}} = 0.5$. The value of 0.2 assigned for a_{CT} and a_{TA} corresponds to low/normal activation levels of the CT/TA muscles, whereas the value $a_{\text{LCA}} = 0.5$ corresponds to the fully adducted VFs with a zero neutral glottal gap, which is typically the case in modal phonation.

The effect of the mask is investigated for a wide range of resistance and mass (inductance) values based on reported values of the scaled mask resistance r_{mask} and scaled mask inductance ρ_{mask} in the literature. The broad range of reported values is likely, in part, due to the array of mask materials studied as well as the differences in the testing methodologies. For example, Drewnick *et al.* (2021) reported values for the mask density ranging from 0.05 to 0.2 kg/m² and mask resistances of 100–1000 Pa s m⁻¹ for a selection of cotton and surgical masks (four surgical mask samples and cotton twill, cotton woven, and jersey cotton samples). Konda *et al.* (2020) reported consistent mask resistance values between 45 and 52 Pa s m⁻¹ for N95, surgical, and cotton masks, whereas Shah *et al.* (2021) reported values ranging from 500 to 800 Pa s m⁻¹ for KN95, R95, and surgical masks without any leakage flow. In this study, the smaller mask resistance measured by Konda *et al.* (2020) was considered reasonable (about 50 Pa s m⁻¹) as the large values reported in other studies would predict unrealistic attenuation in our model. As a result, in our investigation of the influence of the protective measures, we consider the range 0–150 Pa s m⁻¹ for r_{mask} and the range 0–150 g/m² for ρ_{mask} to cover a range from zero to three times the nominal mask values of 50 Pa s m⁻¹ and 50 g/m², respectively. We consider these ranges to capture reasonable variations for the different mask types or the wearing of multiple mask layers. When varying one parameter, resistance or inductance, the other parameter is held fixed at its nominal value.

Because masks and social distancing result in reductions in some voice measures (e.g., intelligibility and sound intensity), we investigate compensating for such deficiencies by means of increasing the static subglottal pressure P_{sub} . It has been found that increasing the subglottal pressure is an efficient mechanism capable of compensating for reductions in the SPL, harmonics-to-noise ratio, and fundamental frequency (Galindo *et al.*, 2017). The range of subglottal pressures considered in this work is 500–6500 Pa in steps of 100 Pa and 6500–9000 Pa in steps of 500 Pa, whereas the static supraglottal pressure P_{sup} is set to be zero (atmospheric). The coarse range 6500–9000 Pa was required to compensate for a large attenuation observed for the vowel /u/ with a mask in combination with social distancing (about 20 dB). We note that such high subglottal pressures are not observed in normal voice clinically but have been observed in shouting (Lagier *et al.*, 2017) and are only included here for completeness.

The simulation outputs considered for analysis are the radiated flow rate q_{rad} , radiated pressure at different distances p_f and the maximum of collision forces between the lower and upper masses $F = \max(F_{\text{col,l}}, F_{\text{col,u}})$ as time vectors. From the time vectors, we compute the means and maxima over time, denoted by $(\cdot)_{\text{mean}}$ and $(\cdot)_{\text{max}}$, respectively. The subscript “0” is used to denote values from the unmasked case, e.g., $P_{\text{sub},0}$ and $q_{\text{rad,mean},0}$. To explore the influence of wearing a mask on the acoustic characteristics of speech, we compute 1 octave band and 1/3 octave band spectra of p_f (using the `p octave` function in MATLAB; MathWorks, 2021) from which the attenuation behaviors are estimated. From the radiated pressure p_f , we estimate the SPL, which is a measure of the sound intensity, and the speech intelligibility index (SII), which correlates with the intelligibility of speech (ANSI, 1997; Hornsby, 2004). Specifically, we compute the SII according to (ANSI, 1997)

$$\text{SII} = \sum_{i=1}^n I_i \max\left(\min\left(\frac{E_i - N_i}{30}, 0\right), 1\right), \quad (5)$$

where i denotes the frequency band, E_i and N_i are the speech and noise spectrum levels (dB), respectively, and I_i is the band importance function. The spectra E_i are computed as spectra from p_f while the pink noise level spectrum is assumed to be 50 dB, roughly comparable to noise levels in hospitals (Busch-Vishniac et al., 2005). To illustrate the effect of noise, we also consider pink noise of 0 and 25 dB.

Because we examine the SII in a nonspecific scenario here, we choose 1/3 octave bands and the average speech band importance function for calculating the SII, where I_i is given by Pavlovic (1987, Table 2) and illustrated in Fig. 2.

IV. PHONATION CHARACTERISTICS WITH MASKS

A. Acoustic effects of masks: Theoretical analysis

In this section, we theoretically analyze the attenuation behavior associated with the mask model introduced in Sec. II B, where, for simplicity, we neglect the coupling with the vocal tract system. Let the complex forward travelling pressure wave amplitude incident on the mask be denoted by \mathbf{p}_{in} and the complex forward travelling pressure wave amplitude

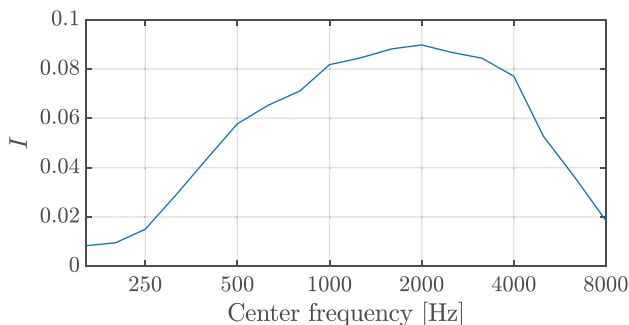


FIG. 2. (Color online) The average band importance function from Pavlovic (1987, Table 2) used for computing the SII.

transmitted at the outlet of the mask be denoted by \mathbf{p}_{out} with both occurring at the frequency ω . By considering the equilibrium of the pressure and velocity on both sides of the mask (Moholkar and Warmoeskerken, 2003), the attenuation ratio, $|\mathbf{p}_{\text{out}}/\mathbf{p}_{\text{in}}|$, can be computed as

$$\left| \frac{\mathbf{p}_{\text{out}}}{\mathbf{p}_{\text{in}}} \right| = \sqrt{\frac{\left(\frac{\omega \rho_{\text{mask}}}{r_{\text{mask}}}\right)^2 + 1}{\left(\omega \rho_{\text{mask}} \left[\frac{1}{r_{\text{mask}}} + \frac{1}{2z_0}\right]\right)^2 + 1}}, \quad (6)$$

where $z_0 = \rho c$ is the characteristic acoustic impedance of air. Let us consider two limiting cases associated with the low and high frequencies. In the case when $\omega \rightarrow 0^+$, the attenuation ratio approaches a value of one (no attenuation). This is because the inductance term acts as a short circuit at zero frequency, resulting in an equivalent resistance of zero. Moreover, using a Taylor expansion at $\omega = 0$, the attenuation behavior at low frequencies can be approximated using the quadratic expression

$$\left| \frac{\mathbf{p}_{\text{out}}}{\mathbf{p}_{\text{in}}} \right| \approx 1 - \frac{1}{2} \left[\left(\frac{1}{r_{\text{mask}}} + \frac{1}{2z_0}\right)^2 - \frac{1}{r_{\text{mask}}^2} \right] \rho_{\text{mask}}^2 \omega^2. \quad (7)$$

Equation (7) shows that at low frequencies, the change in the attenuation behavior is minimal near zero frequency, then as the frequency increases, the attenuation starts to increase more significantly, implying a low-pass filtering behavior. The cutoff frequency associated with the low-pass filtering is given by

$$\omega_c = \frac{2z_0 r_{\text{mask}}}{\rho_{\text{mask}} (r_{\text{mask}} + 2z_0)}. \quad (8)$$

According to Eq. (8), increasing the mask mass density, ρ_{mask} , leads to a decrease in the cutoff frequency, whereas increasing the mask resistance does the opposite.

As $\omega \rightarrow \infty$, the attenuation ratio approaches the asymptotic value,

$$\left| \frac{\mathbf{p}_{\text{out}}}{\mathbf{p}_{\text{in}}} \right|_{\omega \rightarrow \infty} = \frac{1}{\frac{1}{r_{\text{mask}}} + \frac{1}{2z_0}} = \frac{2z_0}{2z_0 + r_{\text{mask}}} \leq 1, \quad (9)$$

which indicates a purely resistive behavior that is independent of the frequency. This implies that at high frequencies, the attenuation is approximately uniform. Equation (9) shows that increasing the mask resistance induces a higher asymptotic attenuation, and that asymptotic attenuation is independent of the mask mass. Figure 3 illustrates a typical attenuation curve of the mask model in this study. The low-pass behavior predicted from the theoretical analysis is in qualitative agreement with experimental observations of the acoustic effects of masks (Corey et al., 2020), which we discuss further in Sec. IV B.

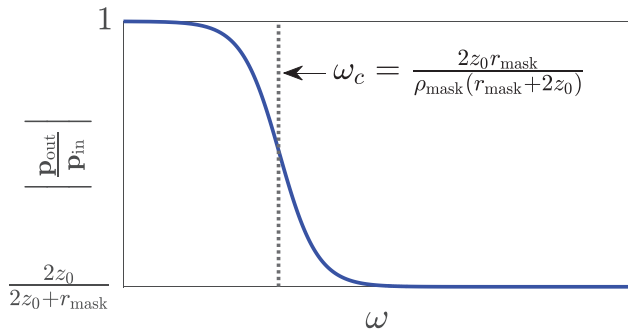


FIG. 3. (Color online) The typical attenuation curve of the mask model.

B. Analysis using phonation simulations

Herein, we look at the influence of masks on the acoustic pressure at a distance of 1 m from the mouth, computed from the phonation simulations using the model introduced in Sec. II (see also Fig. 1). Figure 4 shows the attenuation of the mask, computed using single octave bands as the ratio of the sound intensity with a mask to the sound intensity without, over varying mask parameters (r_{mask} , ρ_{mask}) for different vowels, including the average vowel.

The attenuation curves for most of the vowel sounds show a drop for low frequencies followed by an increase at higher frequencies. The low frequency attenuation and apparent asymptotic behavior at high frequencies are compatible with the theoretical analysis (see Fig. 3). The decrease in the attenuation for the mid range of frequencies in Fig. 4 is apparently due to acoustic coupling between the mask and vocal tract as the mask R-L circuit without a vocal tract is predicted to induce monotonic attenuation behavior (Sec. IV A). The experimental data of the acoustic effects of

masks exhibit low-pass filtering trends on average, however, large variabilities in the attenuation behaviors have been observed. This large variability is attributed to several factors, including the acoustic signals employed, experimental details, and types and mountings of the masks. The data from Corey *et al.* (2020), which are based on analyses of speech signals, predict an almost zero attenuation over the frequency range of approximately 0–1000 Hz for all of the mask types considered. At higher frequencies, attenuation is observed with the degree depending on the mask type and generally leveling off above roughly 4000 Hz. Some of the mask types do, in fact, exhibit slight reductions in the attenuation at the highest frequencies that they considered [see, for example, attenuation of the 2L jersey and 2L denim face coverings in Fig. 3 (right) in Corey *et al.*, 2020)]. This shows that, in general, the predictions from our theoretical and numerical analyses of the attenuation behaviors of masks qualitatively agree with the available experimental data.

Figure 4 also illustrates that mask resistance and inductance affect the attenuation differently. Increasing the mask resistance generally increases the attenuation primarily in the mid to high ranges of the presented frequencies, as appears in the left column of Fig. 4 for most of the vowels. Increasing the mask inductance (mask area density) tends to affect all of the frequencies; see, for example, /i/ in the right column of Fig. 4. This is likely due to acoustic coupling as the pure mask model implies negligible influence of the mask area density at high frequencies. Higher attenuation at low frequencies with an increasing density is expected because increasing the mass decreases the cutoff frequency, which shrinks the low frequency range wherein the mask has negligible effect, in agreement with our theoretical

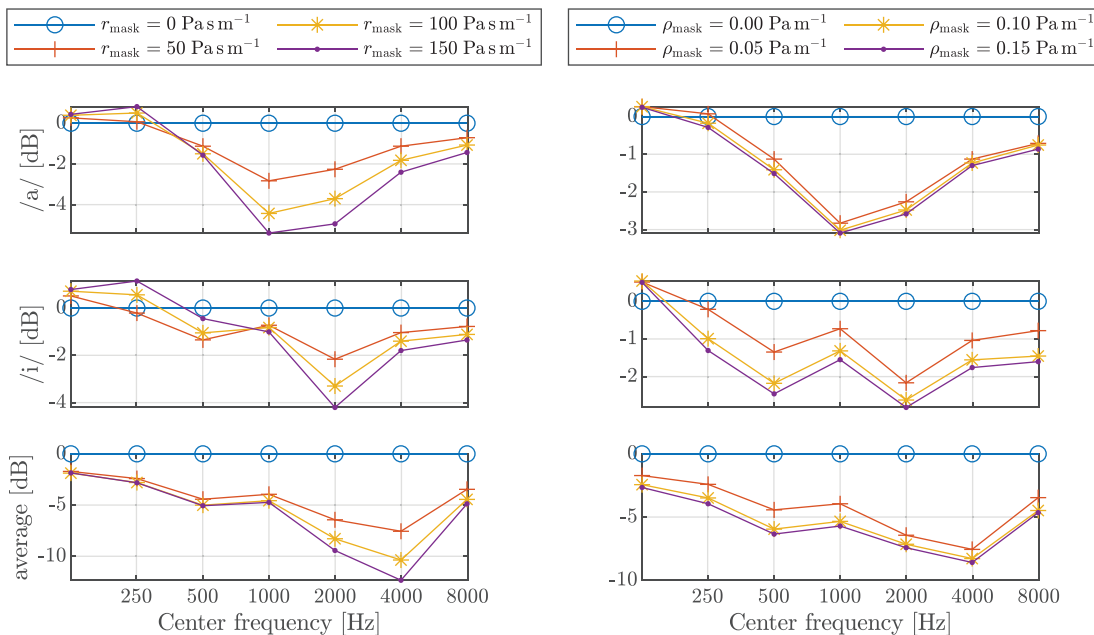


FIG. 4. (Color online) The effect of the mask parameters on sound attenuation for $P_{\text{sub}} = 1000$ Pa are shown with single octave bands. The mask parameters are varied by changing r_{mask} while keeping $\rho_{\text{mask}} = 0.05$ Pa m⁻¹ (left) and changing ρ_{mask} while keeping $r_{\text{mask}} = 50$ Pa s m⁻¹ (right). The attenuation was calculated using p_f at 1 m.

analysis. Furthermore, Fig. 4 (right) shows that the influence of the mask inductance decreases at high values of the area density. This agrees partially with our theoretical analysis as increasing the mask density induces the attenuation to reach its asymptotic limit faster [observe that ω is always multiplied by ρ_{mask} in Eq. (6)]. The frequency dependent behaviors at high area density values further highlight the influence of acoustic coupling on the attenuation as our theoretical analysis, which neglects coupling, predicts uniform attenuation at high frequencies and mask area densities.

Figure 5 presents the SPL, SII, and maximum collision forces as a function of the mask resistance (left) and mass (right) for a selection of vowels in the case of no compensation (that is, at a fixed subglottal pressure). The maximum collision force is normalized by its value with no mask, and the SPL uses the no mask condition as a reference. Figure 5 shows that increasing either the mask resistance or mask density decreases the SII and SPL, which agrees with the day-to-day experience of wearing masks. As in the case of the attenuation curves, the effect of increasing the mask resistance or density varies for different vowels.

The modest reduction in the SII found in Fig. 5 with an increasing mask resistance/inductance generally agrees with the experimental results on the influence of masks on objective intelligibility measures (Palmiero *et al.*, 2016). On the other hand, studies on the influence of masks on intelligibility as measured by the percentage of speech material correctly identified have found mixed effects, where some indicate significant reductions in intelligibility (Keerstock *et al.*, 2020; Toscano and Toscano, 2021; Truong and Weber, 2021) and others note minor effects (Magee *et al.*, 2020). These results do not conflict with the small changes in the SII found here; however, due to the differences in the

experimental conditions (presence of visual cues from mouth motion, background noise, etc.) and because intelligibility, as measured by the percent of speech material understood, does not directly correlate with the SII (Kryter, 1962a,b).

Large decreases in the intelligibility do not necessarily imply large decreases in the SII (articulation index) as intelligibility is insensitive to the SII when it is high and sensitive to the SII when it is low (Kryter, 1962a,b) with the exact relationship depending on additional factors, such as the type of speech sound.

To illustrate this effect in terms of noise, Fig. 6 shows the SII score and corresponding estimated intelligibility (percent of words identified) based on Kryter (1962b, Fig. 15) for the “256 PB words” case. In all of the noise conditions, the effect of the mask on the SII is relatively small with a maximum decrease of about 0.1. As the noise level increases (or the SII in the no mask condition decreases), however, decreases in the corresponding intelligibility due to wearing a mask grow from nearly 0% at a noise level of 0 dB to 20% at a noise level of 50 dB. Therefore, the model investigated here can predict the small and large changes in intelligibility depending on the level of background noise or other factors that decrease the SII in the no mask condition. The experimental studies that found small changes in intelligibility due to a mask were conducted in low noise conditions (Magee *et al.*, 2020), whereas experiments that found large changes in intelligibility due to a mask were conducted in high noise conditions (Keerstock *et al.*, 2020; Toscano and Toscano, 2021; Truong and Weber, 2021).

Figure 5 also displays that as the mask resistance and inductance change, the collision forces are moderately influenced for an average vowel. Specific vowels, however, can

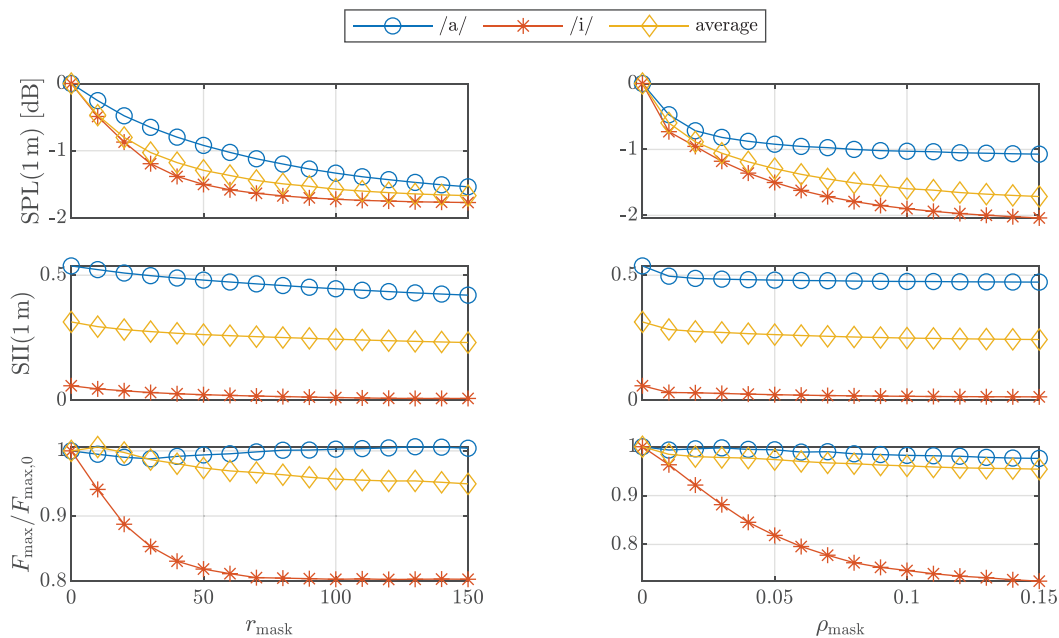


FIG. 5. (Color online) Trends in the BCM model measures for different mask parameters at $P_{\text{sub}} = 1000$ Pa. The background noise is assumed to be 50 dB for the SII calculations. The mask parameters are varied by changing r_{mask} while keeping $\rho_{\text{mask}} = 0.05$ Pa m⁻¹ (left) and changing ρ_{mask} while keeping $r_{\text{mask}} = 50$ Pa s m⁻¹ (right). A subset of investigated vowels has been shown for clarity but all of the vowels are considered in the average vowel case.

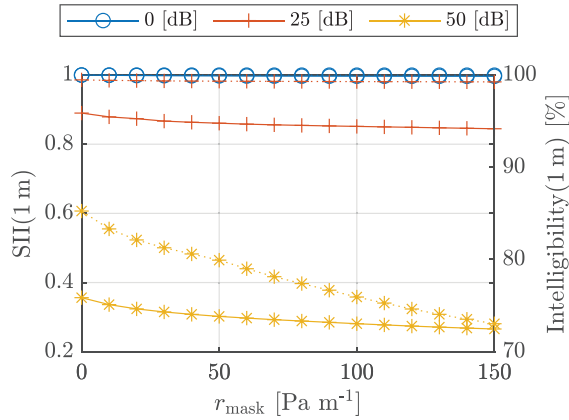


FIG. 6. (Color online) The relation between the SII and intelligibility as a function of the mask resistance at different levels of the background pink noise amplitude for the average vowel at $P_{\text{sub}} = 1000$ Pa. The solid lines indicate the SII, and the dotted lines indicate the corresponding intelligibility.

undergo either increases or decreases in the collision force with an increasing mask resistance/inductance. For example, there is a slight increase in the collision force for the /a/ vowel at $r_{\text{mask}} = 100 \text{ Pa s m}^{-1}$ and a more substantial decrease for the /i/ vowel at $r_{\text{mask}} = 50 \text{ Pa s m}^{-1}$. These changes in the collision force are the result of differing acoustic coupling effects under the increase in mask parameters. Several studies have shown that changes in the acoustic characteristics of the vocal tracts alter the dynamics of the VF oscillations (Lucero *et al.*, 2012; Titze, 2008) with the specific effects depending on a variety of factors, such as the shape of the vocal tract and the resulting distribution of formants.

V. INFLUENCE OF SOCIAL DISTANCING ON ACOUSTIC SIGNALS

In this section, we briefly discuss the influence of social distancing on acoustic signals. Recall the simplified acoustic model of social distancing in Sec. II C and consider the far-field pressure amplitudes associated with the radiated flow rate q_{rad} given in Eq. (3). Let us fix the harmonic index n and consider the pressure amplitudes associated with n at different distances d_1 and d_2 , namely, $p_{f,n}(d_1)$ and $p_{f,n}(d_2)$. Then, using Eq. (3), the ratio of the amplitudes is $|p_{f,n}(d_1)|/|p_{f,n}(d_2)| = d_2/d_1$, which is independent of the frequency ω_n .

Figure 7 displays the influence of increasing the distance on the SPL and SII (assuming 50 dB of background noise). The effect of the distance on the SPL follows a $1/d$ decay regardless of the vowel sound. The effect of the distance on the SII follows a piecewise $1/d$ decay and depends on the vowel sound caused by the saturation effects in the different frequency bands. This inverse relation indicates a reduction in the sound intensity and intelligibility with the distance from the speaker. In Sec. VI, we investigate how compensating for reductions in the voice measures, associated with social distancing and wearing masks, affect the biomechanics of the VFs.

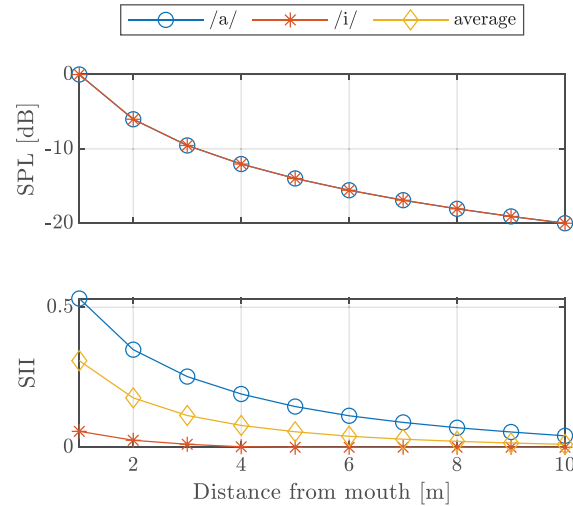


FIG. 7. (Color online) The effect of the distance from the mouth on the SPL and SII for the average vowel at $P_{\text{sub}} = 1000$ Pa. The background noise is assumed to be 50 dB for the SII calculations. The influence of the distance on the SPL is not affected by the vowel tract shapes so all of the results appear identical in the upper plot.

VI. SUBGLOTTAL PRESSURE COMPENSATION

As shown in Secs. IV and V, wearing a mask and social distancing lead to reductions in several acoustic measures, including the SPL and SII. In this section, we aim to explore the influence of increasing the subglottal pressure, P_{sub} , as a compensatory mechanism on the mechanics of phonation, particularly the VF collision forces, which are associated with phonotrauma.

Here, we consider the phonation simulations with increasing mask resistance/mass and various subglottal pressure values. Increasing the mask resistance with the fixed area density corresponds to increasing the mask filtration efficiency while keeping the mass fixed (e.g., wearing a surgical mask instead of a nonmedical mask of the same mass density), whereas increasing the mass density with a fixed resistance corresponds to increasing the thickness/number of layers of the low quality mask to attain a goal filtration efficiency level. For the given SPL and SII in the case of no mask at 1 m, we seek the requisite subglottal pressure that yields the same acoustic output at a given distance when wearing a mask (particular resistance/mass combination). This is performed at 1 and 2 m listener distances to account for the social distancing measures.

Figures 8 and 9 show the compensations in P_{sub} required to achieve the same SPL or SII as in the no mask case at $P_{\text{sub},0} = 1000$ Pa (a reasonable subglottal pressure during speech) for various vowel sounds with an increasing mask resistance and fixed area density and increasing area density and fixed resistance, respectively. For all of the vowels, an increasing mask resistance or mass generally necessitates increasing the subglottal pressure to sustain either the target SPL or SII. Unsurprisingly, doubling the distance from the speaker to the listener also requires an increase in P_{sub} .

The compensation required for the SII and SPL are similar but reflect subtle differences due to their definitions. The

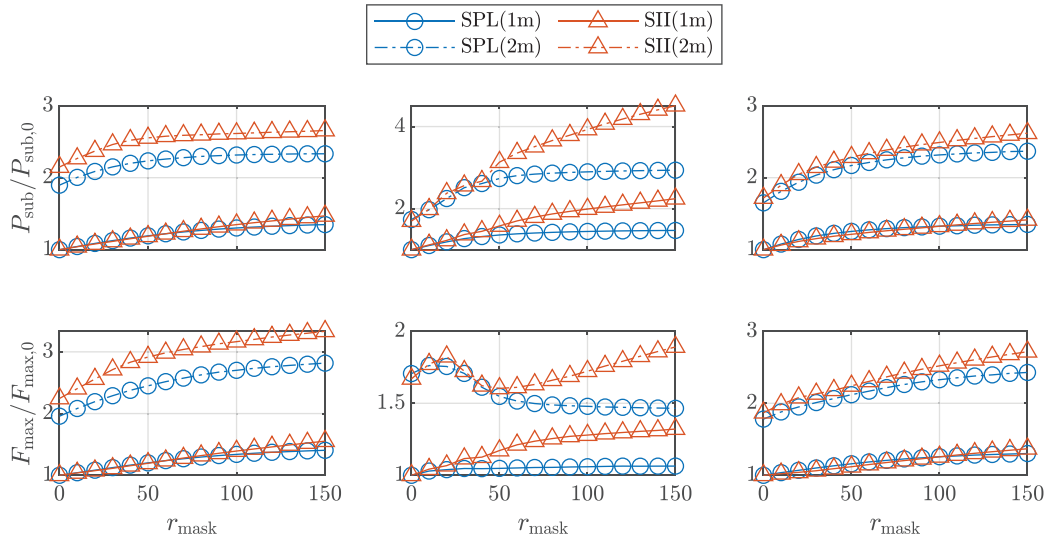


FIG. 8. (Color online) The compensation for the (left) /a/, (middle) /i/, and (right) average vowels as a function of the mask scaled resistance r_{mask} with fixed $\rho_{\text{mask}} = 0.05 \text{ Pa m}^{-1}$. The background noise is assumed to be 50 dB for the SII calculations. (Top row) The subglottal pressure and (bottom row) collision force are shown. The subglottal pressure is normalized by 1000 Pa while F_{max} is normalized by the F_{max} value in the no-mask case. A subset of the investigated vowels has been shown for clarity but all of the vowels are included in the average.

SII is a measure of intelligibility that includes frequency band weighting and saturation effects, whereas the SPL is purely a measure of the sound intensity. As a result, the SPL and SII are affected differently by the frequency dependent attenuation induced by wearing a mask (see Fig. 4) with the compensation required for the SII being generally greater. This is likely because the SII places a greater weight on the mid-band frequencies (Fig. 2), which are typically the frequencies that experience the greatest attenuation by the mask (Fig. 4) in our study.

Herein, the background noise was assumed to be 50 dB to model noise in typical environments, but other noise levels would affect the interpretation of the compensation

results. In low noise environments (when the SII is high in the no mask condition), the minor decreases in the SII due to a mask, shown in Fig. 5 (about 0.1), would have minimal impacts on intelligibility (Kryter, 1962b). This suggests that in low noise environments, the compensation for intelligibility may not be necessary because while the mask does reduce it, the conversation context would likely be sufficient to fill in any gaps. In high noise environments, the SII in the no mask condition will already be low, therefore, the same decrease in the SII results in a much larger decrease in the intelligibility (see Fig. 6). As a result, the full compensatory increase predicted in Figs. 8 and 9 is more applicable. The effect of noise on intelligibility will also depend on

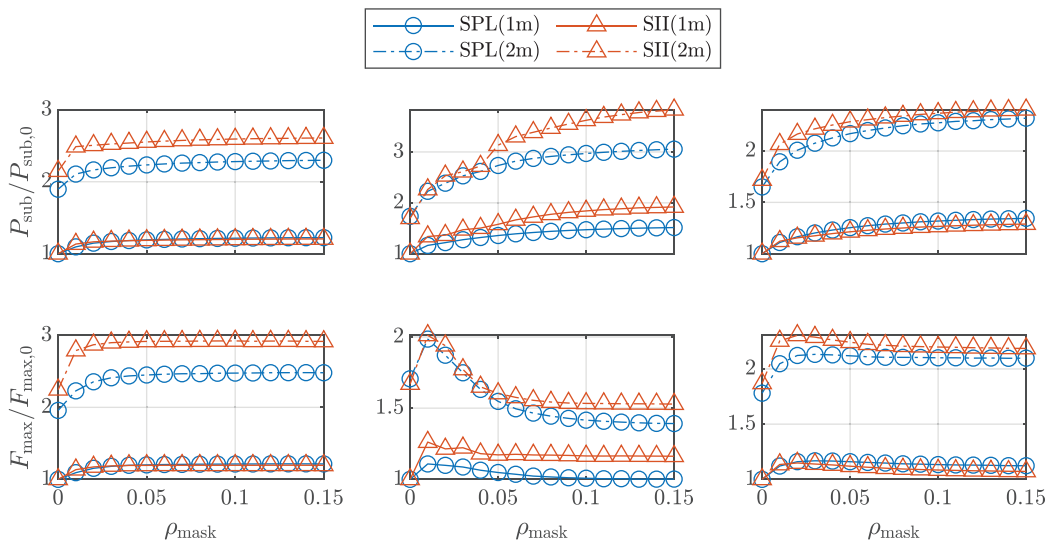


FIG. 9. (Color online) The compensation for the (left) /a/, (middle) /i/, and (right) average vowels as a function of the mask area density ρ_{mask} with fixed $r_{\text{mask}} = 50 \text{ Pa s m}^{-1}$. The background noise is assumed to be 50 dB for the SII calculations. (Top row) The subglottal pressure and (bottom row) collision force are shown. The subglottal pressure is normalized by 1000 Pa while F_{max} is normalized by the F_{max} value in the no-mask case. A subset of investigated vowels has been shown for clarity but all of the vowels are included in the average.

additional factors. For example, [Keerstock et al. \(2020\)](#) found that non-native speaker intelligibility is greatly affected by masks and noise, and using a clear speech style can reduce the effects of masks and noise on intelligibility. Effects like these would influence the relation between the SII and intelligibility and, thus, the level of compensation required.

Figures 8 and 9 show that the compensation required for doubling the distance is generally greater than compensation for increasing the mask resistance or mass, indicating that compensating for social distancing requires a relatively higher vocal effort in comparison with that to overcome the attenuation associated with wearing a mask.

Finally, Figs. 8 and 9 show that increases in the subglottal pressure to compensate for masking and social distancing measures leads to increased VF collision forces.

The trends in the VF collision forces with compensation for different masks and social distancing are caused by a combination of the effect of the mask itself on the collision force and the increased subglottal pressure for compensation. Generally, increasing the subglottal pressure increases the collision forces due to the increased vibration amplitudes; however, increasing the mask resistance/mass can either increase or decrease the collision forces, as seen in Fig. 5, depending on the vowel. In the case of the /a/ vowel, the mask itself has little impact on the collision force so the collision force primarily increases as a result of the increased subglottal pressure for compensation. In the case of the /i/ vowel, increasing the mask resistance/mass tends to decrease the collision force (Fig. 5) while the compensatory effects tend to increase it. As a result, the collision force trends for the /i/ vowel show an initial increase followed by a decrease due to these competing effects.

VII. COMMENTS ON MASK USAGE AND SOCIAL DISTANCING

We observed how compensating for reductions in the different voice measures associated with mask wearing and social distancing alters the mechanics of phonation and, in particular, leads to an increase in the subglottal pressure and VF collision. The collision pressure and resulting high stresses in the VF body have been hypothesized to play a large role in vocal trauma and the formation of VF nodules ([Gunter, 2003](#); [Tao and Jiang, 2007](#); [Titze, 1994](#)). The compensatory subglottal pressure and resulting increased collision forces seen here would likely contribute to an increased risk for vocal hyperfunction, which is in agreement with recent observations of vocal fatigue in healthcare workers who follow protective measures for long periods of time ([McKenna et al., 2021](#)). Forensic investigations on the prevalence of voice pathologies now and in the near future in comparison with pre-pandemic levels will shed additional insight into the clinical repercussions of long term prophylactic use and social distancing, particularly for at risk groups, such as teachers.

Although masks and social distancing can contribute to hyperfunction and the development of voice disorders with

prolonged usage, there are a few practical strategies that could mitigate the deleterious effects of these prophylactics on the voice while retaining their important role in prevention of airborne disease transmission. First, light masks are preferable to heavy masks for the same particle filtration properties. This is because the larger mask mass increases the sound attenuation and will require larger compensatory effects. Second, the negative effects of masks on intelligibility can be greatly reduced by speaking in low noise environments. When intelligibility is high, mask wearing causes only minor decreases in intelligibility such that compensation may not be required (Sec. VI). As speech intelligibility can be increased also by reducing the distance between the speaker and audience, there are practical considerations in certain environments that could reduce fatigue. For example, seating configurations can be adjusted such that the distance from the speaker to the audience is similar for all of the audience members (e.g., put classrooms' desks in a circular arrangement to follow social distancing guidelines while simultaneously minimizing the distance to the furthest listener). Additionally, microphones should be employed when possible to eliminate the need of a speaker to raise their voice. Intelligibility can also be increased by changing the speech style, such as by speaking in a clear style ([Keerstock et al., 2020](#)). Combined, these strategies could greatly reduce the compensatory adjustments required while wearing a mask and maintaining a safe social distance.

VIII. LIMITATIONS

The current study aimed to investigate the consequences of following two of the recommended COVID-19 protective measures, namely, social distancing and mask wearing, on the biomechanics of phonation. Although our analysis was effective in revealing some of the potential consequences of the protective measures on the vocal health of individuals, the extent of the applicability of the results from the analysis is limited due to the implemented assumptions, for example, the use of a simplified acoustic model of social distancing, which neglects the frequency dependent effects. These may influence how the distance affects intelligibility especially if large distances are to be considered, neglecting the effects of the surroundings (walls, ceiling, corners) on acoustic signals (reflection, absorption, interference) and how such effects influence intelligibility and acoustic attenuation associated with COVID-19 protective measures, and considering the SII and SPL only when studying compensation. Our measurement of intelligibility through SII, also, cannot capture some aspects of intelligibility; for example, context, body language, and phrasing in real speech could help improve intelligibility despite poor intelligibility from the acoustics alone. There are several vocal and nonvocal measures (such as the effects on breathing and mouth visibility) that are affected by the COVID-19 protective measures, and the compensation patterns associated with these other measures may be different. However, it is unclear what vocal and nonvocal measures besides

“being heard” are compensated for in individuals when mask wearing and social distancing. Our usage of a subset of vowel sounds to represent average speech may also be limited as we observed in Sec. IV B that acoustic coupling has a significant effect on the attenuation behavior of masks. As a result, it may be important to consider running speech and consonant sounds to elucidate more accurately the acoustic effects of COVID-19 protective measures, especially mask wearing, on vocal health.

IX. CONCLUSION

In this paper, by means of numerical phonation simulations, we investigated the effects of wearing masks and social distancing on intelligibility and sound intensity. Moreover, we studied how compensating for reductions in the SII and SPL by means of increasing the subglottal pressure affects the mechanics of phonation.

Our analysis showed that masks have low-pass filtering effects, which agrees qualitatively with the available experimental observations. Furthermore, numerical simulations demonstrated how wearing masks and social distancing reduce the sound intensity and intelligibility. The simulations showed that decreases in the SII and SPL due to the mentioned protocols require compensatory subglottal pressure increases. These compensatory increases could potentially lead to vocal hyperfunction and, in turn, the development of other vocal disorders such as nodules.

The current study employed a simple acoustic model of masks that captures the general trends reasonably while there are some deviations from experimental observations of the acoustic effects of masks. In future work, we aim to develop and implement models that capture the acoustic effects of masks more accurately. Then, such models will be used in phonation simulations to weigh the significance of increased VF collision pressures associated with compensating for reduced voice measures to analyze the long term effects of wearing masks on the health of the VFs.

ACKNOWLEDGMENTS

The research reported in this work was supported, in part, by the National Institute on Deafness and Other Communication Disorders (NIDCD) of the National Institutes of Health (NIH) under Award No. P50DC015446, the National Science Foundation (CBET:2029548), and Agencia Nacional de Investigación y Desarrollo (ANID) under Award No. BASAL FB0008. The content is solely the responsibility of the authors and does not necessarily represent the official views of the NIH. J.J.D. and M.A.S. contributed equally to this paper.

¹In this study, we define a mask to be any thin porous textile material. This definition covers a wide variety of mask types, including surgical masks, nonmedical masks, and cloth face covers. As modeling assumptions, the flow through a mask is assumed to be proportional to the pressure difference across the mask when the mask mass is at rest, and the mask dynamics are driven by that pressure difference (see Sec. II B).

Agrawal, A., and Bhardwaj, R. (2020). “Reducing chances of COVID-19 infection by a cough cloud in a closed space,” *Phys. Fluids* **32**(10), 101704.

ANSI (1997). S3.5. *American National Standard Methods for Calculation of the Speech Intelligibility Index* (Acoustical Society of America, Melville, NY).

Attenborough, K. (2014). *Sound Propagation in the Atmosphere* (Springer, New York), pp. 117–155.

Busch-Vishniac, I. J., West, J. E., Barnhill, C., Hunter, T., Orellana, D., and Chivukula, R. (2005). “Noise levels in Johns Hopkins Hospital,” *J. Acoust. Soc. Am.* **118**(6), 3629–3645.

Carbon, C.-C. (2020). “Wearing face masks strongly confuses counterparts in reading emotions,” *Front. Psychol.* **11**, 2526.

Corey, R. M., Jones, U., and Singer, A. C. (2020). “Acoustic effects of medical, cloth, and transparent face masks on speech signals,” *J. Acoust. Soc. Am.* **148**(4), 2371–2375.

Dejonckere, P. H., and Kob, M. (2009). “Pathogenesis of vocal fold nodules: New insights from a modelling approach,” *Folia Phoniatr. Logop.* **61**(3), 171–179.

Drewnick, F., Pikmann, J., Fachinger, F., Moormann, L., Sprang, F., and Borrmann, S. (2021). “Aerosol filtration efficiency of household materials for homemade face masks: Influence of material properties, particle size, particle electrical charge, face velocity, and leaks,” *Aerosol Sci. Technol.* **55**(1), 63–79.

Eikenberry, S. E., Mancuso, M., Iboi, E., Phan, T., Eikenberry, K., Kuang, Y., Kostelich, E., and Gumel, A. B. (2020). “To mask or not to mask: Modeling the potential for face mask use by the general public to curtail the COVID-19 pandemic,” *Infect. Dis. Modell.* **5**, 293–308.

Evans, L., Bass, H., and Sutherland, L. (1972). “Atmospheric absorption of sound: Theoretical predictions,” *J. Acoust. Soc. Am.* **51**(5B), 1565–1575.

Flanagan, J. L., Ishizaka, K., and Shipley, K. (1975). “Synthesis of speech from a dynamic model of the vocal cords and vocal tract,” *Bell Syst. Tech. J.* **54**(3), 485–506.

Galindo, G. E., Peterson, S. D., Erath, B. D., Castro, C., Hillman, R. E., and Zaňartu, M. (2017). “Modeling the pathophysiology of phonotraumatic vocal hyperfunction with a triangular glottal model of the vocal folds,” *J. Speech. Lang. Hear. Res.* **60**(9), 2452–2471.

Galindo, G. E., Zanartu, M., and Yuz, J. I. (2014). “A discrete-time model for the vocal folds,” in *IEEE Engineering in Medicine and Biology Society International Student Conference*, Citeseer, pp. 74–77.

Gunter, H. E. (2003). “A mechanical model of vocal-fold collision with high spatial and temporal resolution,” *J. Acoust. Soc. Am.* **113**(2), 994–1000.

Guss, J., Sadoughi, B., Benson, B., and Sulica, L. (2014). “Dysphonia in performers: Toward a clinical definition of laryngology of the performing voice,” *J. Voice* **28**(3), 349–355.

Hadwin, P. J., Galindo, G. E., Daun, K. J., Zaňartu, M., Erath, B. D., Cataldo, E., and Peterson, S. D. (2016). “Non-stationary Bayesian estimation of parameters from a body cover model of the vocal folds,” *J. Acoust. Soc. Am.* **139**(5), 2683–2696.

Hayden, R. E. (1950). “The relative frequency of phonemes in general-American English,” *WORD* **6**(3), 217–223.

Hillman, R. E., Holmberg, E. B., Perkell, J. S., Walsh, M., and Vaughan, C. (1989). “Objective assessment of vocal hyperfunction: An experimental framework and initial results,” *J. Speech. Lang. Hear. Res.* **32**(2), 373–392.

Hillman, R. E., Stepp, C. E., Van Stan, J. H., Zaňartu, M., and Mehta, D. D. (2020). “An updated theoretical framework for vocal hyperfunction,” *Am. J. Speech. Lang. Pathol.* **29**, 2254–2257.

Hornsby, B. W. (2004). “The Speech Intelligibility Index: What is it and what’s it good for?,” *Hear. J.* **57**(10), 10–17.

Ishizaka, K., and Flanagan, J. L. (1972). “Synthesis of voiced sounds from a two-mass model of the vocal cords,” *Bell Syst. Tech. J.* **51**(6), 1233–1268.

ISO (1993). 9613-1, “Acoustics—Attenuation of sound during propagation outdoors—Part 1: Calculation of the absorption of sound by the atmosphere” (International Organization for Standardization, Geneva, Switzerland).

Jiang, J. J., Diaz, C. E., and Hanson, D. G. (1998). “Finite element modeling of vocal fold vibration in normal phonation and hyperfunctional dysphonia: Implications for the pathogenesis of vocal nodules,” *Ann. Otol. Rhinol. Laryngol.* **107**(7), 603–610.

- Keerstock, S., Meemann, K., Ransom, S. M., and Smiljanic, R. (2020). "Effects of face masks and speaking style on audio-visual speech perception and memory," *J. Acoust. Soc. Am.* **148**(4), 2747.
- Kelly, J. L., and Lochbaum, C. C. (1962). "Speech synthesis," in *Proceedings of the Fourth International Congress on Acoustics*.
- Khosronejad, A., Santoni, C., Flora, K., Zhang, Z., Kang, S., Payabvash, S., and Sotiropoulos, F. (2020). "Fluid dynamics simulations show that facial masks can suppress the spread of COVID-19 in indoor environments," *AIP Adv.* **10**(12), 125109.
- Kinsler, L. E., Frey, A. R., Coppens, A. B., and Sanders, J. V. (1999). *Fundamentals of Acoustics* (Wiley, New York).
- Konda, A., Prakash, A., Moss, G. A., Schmoltd, M., Grant, G. D., and Guha, S. (2020). "Aerosol filtration efficiency of common fabrics used in respiratory cloth masks," *ACS Nano* **14**(5), 6339–6347.
- Koyama, T., Weeraratne, D., Snowdon, J. L., and Parida, L. (2020). "Emergence of drift variants that may affect COVID-19 vaccine development and antibody treatment," *Pathogens* **9**(5), 324.
- Kryter, K. D. (1962a). "Methods for the calculation and use of the articulation index," *J. Acoust. Soc. Am.* **34**(11), 1689–1697.
- Kryter, K. D. (1962b). "Validation of the articulation index," *J. Acoust. Soc. Am.* **34**(11), 1698–1702.
- Lagier, A., Legou, T., Galant, C., Amy de La Bretèque, B., Meynadier, Y., and Giovanni, A. (2017). "The shouted voice: A pilot study of laryngeal physiology under extreme aerodynamic pressure," *Logoped. Phoniater. Vocol.* **42**(4), 141–145.
- Liljencrants, J. (1985). "Speech synthesis with a reflection-type line analog," Ph.D. thesis, Royal Institute of Technology, Stockholm.
- Lucero, J. C., Lourenço, K. G., Hermant, N., Van Hirtum, A., and Pelorsson, X. (2012). "Effect of source–tract acoustical coupling on the oscillation onset of the vocal folds," *J. Acoust. Soc. Am.* **132**(1), 403–411.
- Lucero, J. C., and Schoentgen, J. (2015). "Smoothness of an equation for the glottal flow rate versus the glottal area," *J. Acoust. Soc. Am.* **137**(5), 2970–2973.
- Magee, M., Lewis, C., Noffs, G., Reece, H., Chan, J. C., Zaga, C. J., Paynter, C., Birchall, O., Rojas Azocar, S., Ediriweera, A., Kenyon, K., Caverlé, M. W., Schultz, B. G., and Vogel, A. P. (2020). "Effects of face masks on acoustic analysis and speech perception: Implications for peripandemic protocols," *J. Acoust. Soc. Am.* **148**(6), 3562–3568.
- MathWorks (2021). "Generate octave spectrum—MATLAB octave," available at <https://www.mathworks.com/help/signal/ref/poctave.html> (Last viewed September 15, 2021).
- McKenna, V. S., Patel, T. H., Kendall, C. L., Howell, R. J., and Gustin, R. L. (2021). "Voice acoustics and vocal effort in mask-wearing healthcare professionals: A comparison pre-and post-workday," *J. Voice* (published online).
- Mheidly, N., Fares, M. Y., Zalzale, H., and Fares, J. (2020). "Effect of face masks on interpersonal communication during the COVID-19 pandemic," *Front. Public Health* **8**, 582191.
- Mittal, R., Ni, R., and Seo, J.-H. (2020). "The flow physics of COVID-19," *J. Fluid Mech.* **894**, F2.
- Moholkar, V. S., and Warmoeskerken, M. M. (2003). "Acoustical characteristics of textile materials," *Text. Res. J.* **73**(9), 827–837.
- Ndwandwe, D., and Wiysonge, C. S. (2021). "COVID-19 vaccines," *Curr. Opin. Immunol.* **71**, 111–116.
- Palmiero, A. J., Symons, D., Morgan, J. W., III, and Shaffer, R. E. (2016). "Speech intelligibility assessment of protective facemasks and air-purifying respirators," *J. Occup. Environ. Hyg.* **13**(12), 960–968.
- Pavlovic, C. V. (1987). "Derivation of primary parameters and procedures for use in speech intelligibility predictions," *J. Acoust. Soc. Am.* **82**(2), 413–422.
- Pieren, R. (2012). "Sound absorption modeling of thin woven fabrics backed by an air cavity," *Text. Res. J.* **82**(9), 864–874.
- Qian, M., and Jiang, J. (2022). "COVID-19 and social distancing," *J. Public Health (Berl.)* **30**, 259–261.
- Roy, N., Merrill, R. M., Thibeault, S., Parsa, R. A., Gray, S. D., and Smith, E. M. (2004). "Prevalence of voice disorders in teachers and the general population," *J. Speech Lang. Hear. Res.* **47**, 281–293.
- Saunders, G. H., Jackson, I. R., and Visram, A. S. (2021). "Impacts of face coverings on communication: An indirect impact of COVID-19," *Int. J. Audiol.* **60**(7), 495–506.
- Serry, M. A., Stepp, C. E., and Peterson, S. D. (2021). "Physics of phonation offset: Towards understanding relative fundamental frequency observations," *J. Acoust. Soc. Am.* **149**(5), 3654–3664.
- Shah, Y., Kurelek, J. W., Peterson, S. D., and Yarusevych, S. (2021). "Experimental investigation of indoor aerosol dispersion and accumulation in the context of COVID-19: Effects of masks and ventilation," *Phys. Fluids* **33**(7), 073315.
- Sommer, D. E., Erath, B. D., Zanartu, M., and Peterson, S. D. (2012). "Corrected contact dynamics for the Steinecke and Herzog asymmetric two-mass model of the vocal folds," *J. Acoust. Soc. Am.* **132**(4), EL271–EL276.
- Sommer, D. E., Erath, B. D., Zaňartu, M., and Peterson, S. D. (2013). "The impact of glottal area discontinuities on block-type vocal fold models with asymmetric tissue properties," *J. Acoust. Soc. Am.* **133**(3), EL214–EL220.
- Steinecke, I., and Herzog, H. (1995). "Bifurcations in an asymmetric vocal-fold model," *J. Acoust. Soc. Am.* **97**(3), 1874–1884.
- Story, B. H. (1995). "Physiologically-based speech simulation using an enhanced wave-reflection model of the vocal tract," Ph.D. thesis, University of Iowa, Iowa City, IA.
- Story, B. H. (2005). "A parametric model of the vocal tract area function for vowel and consonant simulation," *J. Acoust. Soc. Am.* **117**(5), 3231–3254.
- Story, B. H., and Titze, I. R. (1995). "Voice simulation with a body-cover model of the vocal folds," *J. Acoust. Soc. Am.* **97**(2), 1249–1260.
- Story, B. H., Titze, I. R., and Hoffman, E. A. (1998). "Vocal tract area functions for an adult female speaker based on volumetric imaging," *J. Acoust. Soc. Am.* **104**(1), 471–487.
- Takemoto, H., Honda, K., Masaki, S., Shimada, Y., and Fujimoto, I. (2006). "Measurement of temporal changes in vocal tract area function from 3D cine-MRI data," *J. Acoust. Soc. Am.* **119**(2), 1037–1049.
- Tao, C., and Jiang, J. J. (2007). "Mechanical stress during phonation in a self-oscillating finite-element vocal fold model," *J. Biomech.* **40**(10), 2191–2198.
- Titze, I., and Alipour, F. (2006). *The Myoelastic-Aerodynamic Theory of Phonation* (National Center for Voice and Speech, Iowa City, IA).
- Titze, I. R. (1984). "Parameterization of the glottal area, glottal flow, and vocal fold contact area," *J. Acoust. Soc. Am.* **75**(2), 570–580.
- Titze, I. R. (1994). "Mechanical stress in phonation," *J. Voice* **8**(2), 99–105.
- Titze, I. R. (2008). "Nonlinear source-filter coupling in phonation: Theory," *J. Acoust. Soc. Am.* **123**(5), 2733–2749.
- Titze, I. R., and Story, B. H. (2002). "Rules for controlling low-dimensional vocal fold models with muscle activation," *J. Acoust. Soc. Am.* **112**(3), 1064–1076.
- Toscano, J. C., and Toscano, C. M. (2021). "Effects of face masks on speech recognition in multi-talker babble noise," *PLoS One* **16**(2), e0246842.
- Truong, T. L., and Weber, A. (2021). "Intelligibility and recall of sentences spoken by adult and child talkers wearing face masks," *J. Acoust. Soc. Am.* **150**(3), 1674–1681.
- Weibel, E. R. (1963). *Morphometry of the Human Lung* (Springer, New York).
- Xie, X., Li, Y., Chwang, A., Ho, P., and Seto, W. (2007). "How far droplets can move in indoor environments—Revisiting the wells evaporation-falling curve," *Indoor Air* **17**(3), 211–225.
- Zaňartu, M. (2006). "Influence of acoustic loading on the flow-induced oscillations of single mass models of the human larynx," Master's thesis, Purdue University, West Lafayette, IN.
- Zaňartu, M., Galindo, G. E., Erath, B. D., Peterson, S. D., Wodicka, G. R., and Hillman, R. E. (2014). "Modeling the effects of a posterior glottal opening on vocal fold dynamics with implications for vocal hyperfunction," *J. Acoust. Soc. Am.* **136**(6), 3262–3271.
- Zaňartu, M., Mongeau, L., and Wodicka, G. R. (2007). "Influence of acoustic loading on an effective single mass model of the vocal folds," *J. Acoust. Soc. Am.* **121**(2), 1119–1129.
- Zhang, Y., and Jiang, J. J. (2004). "Chaotic vibrations of a vocal fold model with a unilateral polyp," *J. Acoust. Soc. Am.* **115**(3), 1266–1269.